



Stabilization of a cantilever pipe conveying fluid using electromagnetic actuators of the transformer type

Tomasz Szmidt · Robert Konowrocki · Dominik Pisarski

Received: 14 May 2021 / Accepted: 13 August 2021 / Published online: 28 August 2021
© The Author(s) 2021

Abstract The article presents an investigation of the stabilization of a cantilever pipe discharging fluid using electromagnetic actuators of the transformer type. With the flow velocity reaching a critical value, the straight equilibrium position of the pipe becomes unstable, and self-excited lateral vibrations arise. Supplying voltage to the actuators yields two opposite effects. First, each of the actuators attracts the pipe, thus introduces the effect of negative stiffness which destabilizes the middle equilibrium. Second, lateral vibrations change the gap in magnetic circuits of the actuators, which leads to oscillations of magnetic field in the cores and the electromagnetic phenomena of induction and hysteresis that impede the motion of the pipe. The combination of these two non-linear effects is ambiguous, so the problem is explored both theoretically and experimentally. First, a mathematical model of the system in form of a partial differential equation governing the dynamics of the pipe coupled with two ordinary differential equations of electromagnetodynamics of the actuators is presented. Then, the equation of the pipe's dynamics is discretized using the Galerkin procedure, and the resultant set of ordinary equations is solved numerically. It has been shown that the overall effect of actuators action is

positive: the critical flow velocity has been increased and the amplitude of post-critical vibrations reduced. These results have been validated experimentally on a test stand.

Keywords Fluid-structure interaction · Pipe · Flow · Dynamic stability · Electromagnetic actuator

1 Introduction

The problem of dynamics of fluid-conveying pipes has been investigated for numerous reasons. Such pipes are widely encountered in engineering applications such as cooling systems, pipelines, aerial refueling operations, ocean mining, so the results of research works may find practical applications [19, 21, 35]. Another reason is that it has become a model dynamical problem [28] which may be used as a tool for understanding the dynamics of more complex systems and a way in searching new phenomena and new dynamical features.

Consider a cantilever pipe with flow. When the flow velocity is high enough, the steady equilibrium position becomes unstable and self-excited lateral vibrations appear [16]. This phenomenon can be easily observed in a loose garden hose conveying water in which momentum flux causes the follower thrust and a snake-like motion of the free end. Moreover, such

T. Szmidt (✉) · R. Konowrocki · D. Pisarski
Institute of Fundamental Technological Research, Polish
Academy of Sciences, Pawińskiego 5B,
02-106 Warszawa, Poland
e-mail: tszmidt@ippt.pan.pl

behavior is specific to cantilever support (pipes with both ends supported undergo a buckling-type of instability) [2].

Pipes with flow are an example of non-conservative elastic systems subjected to a follower load, i.e. a load that constantly remains tangential to pipe's longitudinal axis. Such systems are susceptible even to small changes of physical parameters and to the introduction of new effects (e.g. damping) [12]. A viscous-type external and internal damping, additional point mass or permanent magnets can decrease the critical flow velocity as well as stabilize the system [7, 17, 33]. Critical flow velocity is also affected by the type of foundation [13, 43] and the application of intermediate supports [22, 34]. Moreover, the destabilizing effect of damping has attracted attention of the researchers due to its possible application for energy harvesting [29].

In recent years, functionally graded materials have attracted the attention of the researchers due to their ability to improve dynamical properties of pipes with internal flow. The studies include enhancing the dynamic stability of such systems [44], stabilization of multi-span spinning pipes conveying fluid [23], dynamics of a spinning pipe with its free end operating in a high temperature environment [11] or subjected to temperature changes [8].

Numerous active control methods have been proposed to stabilize fluid-conveying pipes. They rely on the concept of applying various devices to generate transverse forces or bending moments that affect the system in an active way. Examples include the use of servomotors connected to a pipe in some way [5, 9, 40], gyroscopic mechanisms [6], and piezoelectric elements attached to a pipe [14, 24, 42].

Despite their efficiency, active methods can destabilize the system if a failure occurs since the action of forces or moments can introduce additional energy into the system. Thus, in our research works we focus on the use of semi-active methods. In order to stabilize the pipe conveying fluid, electromagnetic phenomena may be applied. For this, two distinctively different methods can be used. *Motional* actuator, a.k.a. a Lorentz type of an electromagnetic device [15, 41] consists of a conductive plate attached to the pipe and moving with it within perpendicular magnetic field. This motion induces eddy currents in plates and a drag force resulting from the Lenz law. Such devices have found numerous applications, for example in vehicle suspension systems [10], beam structures [45] or

elevators and other rail systems where they act as electromagnetic brakes [26]. In our previous works we analyzed the effect of electromagnetic devices of the motional type to stabilize a fluid-conveying pipe which proved to be efficient when used both in passive way as well as in a closed-loop feedback control, depending on the state of the system [30, 36].

In this work we focus on another type of electromagnetic devices, namely the *transformer* actuators. In their case ferromagnetic cores are embedded in the pipe, and the system is placed between two electromagnets. When the voltage is applied, each of the actuators pulls the pipe, thus exerts the effect which destabilizes the middle equilibrium. On the other hand, lateral vibrations change the gap in magnetic circuits, which leads to oscillations of magnetic field in the cores, and consequently, the electromagnetic phenomena of induction and hysteresis, which cause the passive effect impeding the motion. These variations of magnetic flux passing through the cores are the reason to call this actuator the transformer device, also known as the Maxwell device [15, 41].

Transformer actuators are widely used in active magnetic bearings, where they stabilize magnetic levitation of the rotor within the gap [32]. They can also be applied for improving dynamical properties of shafts supported by hydrodynamic bearings [1]. Graves *et al.* compared performance of transformer and motional devices for a given magnetic field and given volume of conducting material. According to the authors, in certain range of dimensions, the transformer device can be more efficient, but in most realistic situations, motional devices have greater efficiency [15].

The combination of negative stiffness and damping of electromagnetic origin generated by transformer devices, both of which depend in a non-linear way on the structure's displacement and velocity, exerts an ambiguous effect that influences the system dynamics – its stability and the critical flow velocity. It has been shown numerically that the overall effect may be positive, i.e. the critical flow velocity may be increased [37]. However, those results showed rather mediocre performance of the actuators. Moreover, the theoretical predictions have not been validated experimentally. Therefore we explore this problem further and verify the result on a specially designed test stand.

The paper is structured as follows. First, we describe the system and its dynamical model. Then, numerical simulations that show its key dynamical features are presented. Finally, after the description of the laboratory set-up, experimental results that validate numerical simulations are presented.

2 Dynamic model

2.1 Governing equations

In this section the dynamics of a cantilever pipe with electromagnetic actuators of the transformer type will be investigated. The pipe is mounted vertically in a clamped configuration and the fluid is discharged from the free end, see Fig. 1.

A complete dynamical model of fluid-conveying pipes involves non-linear phenomena [25, 39]. However, according to author’s previous research works, the non-linearity introduced by the electromagnetic force generated by the transformer devices is much more important for dynamics of a similar elastic structure with a follower force – Beck’s column – than the geometrical one [38]. Taking into account that the pipe is slender and it is subjected to small lateral oscillations in the plane of symmetry $\xi - w$, it can be assumed that the linear Bernoulli-Euler model is valid.

Denote the horizontal deflection of the pipe by $w = w(\xi, t)$. A material damping of the viscous type is included. The gravity force is passed over as its influence on dynamics is well known. The mass of the

actuators is incorporated in the model in a lumped form, but their rotatory inertia is disregarded. This is justified since the steel plates attached to the pipe are short compared to the length of the structure. The so called plug flow model is assumed, which means that the flow velocity is constant in every cross-section perpendicular to the longitudinal axis of the pipe.

The set of equations governing the dynamics of the system is as follows:

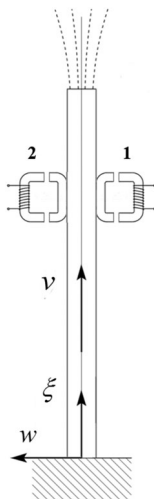
$$\begin{aligned}
 EI \frac{\partial^4 w}{\partial \xi^4} + E^* I \frac{\partial^5 w}{\partial \xi^4 \partial t} + m_f v^2 \frac{\partial^2 w}{\partial \xi^2} + 2m_f v \frac{\partial^2 w}{\partial \xi \partial t} \\
 + (m + m_f + M_a \delta_a) \frac{\partial^2 w}{\partial t^2} = \frac{A}{\mu_0} (B_2^2 - B_1^2) \delta_a \\
 \left(\frac{AN^2}{R} + \frac{1}{8} \sigma l a^2 \right) \frac{dB_{1,2}}{dt} + \frac{2}{\mu_0} (z^* \pm w(\xi_a, t)) B_{1,2} \\
 + \frac{l}{\mu_r \mu_0} B_{1,2} = \frac{NU}{R},
 \end{aligned} \tag{1}$$

where L is the pipe’s length, EI and E^*I – the bending stiffness and bending damping of the pipe, m and m_f – the masses (per unit length) of the pipe and the fluid, M_a – the mass of the actuators attached at the distance ξ_a from the pipe’s support, v – the flow velocity, δ_a – the Dirac delta function concentrated at ξ_a , $B_1 = B_1(t)$ and $B_2 = B_2(t)$ – the magnetic inductions in the electromagnets’ circuits, $l, A = \pi a^2, \sigma$ – the length, circular cross-section area and electrical conductivity of magnetic circuits, N, R – the number and electrical resistance of the electromagnets’ coils, U – the constant voltage supplied to the electromagnets, μ_0, μ_r – the relative magnetic permeability of the vacuum and the ferromagnetic material of the cores, and z^* – the gap between the actuators and the pipe. Number „1” denotes the actuator located at the negative part of the deflection axis, „2” stands for the other actuator.

The clamped support yields the following boundary conditions

$$\begin{aligned}
 w|_{\xi=0} = \frac{\partial w}{\partial \xi} \Big|_{\xi=0} = \left(EI \frac{\partial^2 w}{\partial \xi^2} + E^* I \frac{\partial^3 w}{\partial \xi^2 \partial t} \right)_{\xi=L} \\
 = \left(EI \frac{\partial^3 w}{\partial \xi^3} + E^* I \frac{\partial^4 w}{\partial \xi^3 \partial t} \right)_{\xi=L} = 0.
 \end{aligned} \tag{2}$$

Fig. 1 Investigated system – standing cantilever pipe conveying fluid with electromagnetic devices of the transformer type



The linear partial differential equation of pipe’s dynamics is similar to the equation that was validated years ago [27]. What sets them apart is the incorporation of internal damping in the pipe and the effect of the actuators – their mass and electromagnetic force acting on the pipe. This equation is also similar to the equation used by the authors in the research on dynamics and control of the pipe with motional actuators [36]. The only difference is that instead of the term expressing the electromagnetic viscous drag, the right hand side of the equation contains the expression for the electromagnetic force $F(t) = \frac{A}{\mu_0} (B_2^2 - B_1^2)$ generated by the devices of the transformer type. The term $F(t)$ couples the PDE with the non-linear ordinary differential equations governing the electro-magnetodynamics of the actuators [38].

Note that the self-excited vibrations of the pipe are a result of two opposite effects generated by the flow. One is the inertial force of the moving fluid $m_f v^2 \partial^2 w / \partial \xi^2$, which is an equivalent to the follower force in Beck’s problem and destabilizes the system. The other is the Coriolis force $2m_f v \partial^2 w / \partial \xi \partial t$, which exerts a damping effect.

2.2 Galerkin’s discretization

In this section numerical simulations will be conducted by means of a discretized system represented by a set of ordinary differential equations. Assume an approximate solution to the partial differential Eq. (1) in form of a linear combination of cantilever’s eigenfunctions

$$w(\xi, t) = \sum_{j=1}^n W_j(\xi) Y_j(t), \tag{3}$$

$$W_j(\xi) = C_j \left[\cosh \frac{\lambda_j}{L} \xi - \cos \frac{\lambda_j}{L} \xi + \frac{\sin \lambda_j - \sinh \lambda_j}{\cos \lambda_j + \cosh \lambda_j} \left(\sinh \frac{\lambda_j}{L} \xi - \sin \frac{\lambda_j}{L} \xi \right) \right], \tag{4}$$

where λ_j are the consecutive roots of the characteristic equation $\cos \lambda \cosh \lambda = -1$, and C_j – the constants that normalize the modal shapes with respect to the norm generated by the scalar product $\int_0^L W_i W_j$. As a result of Galerkin procedure a set of n second-order ODE’s for

the vector of unknown generalized coordinates $\mathbf{Y} = (Y_i)_{n \times 1}$ is obtained

$$\mathbf{M} \ddot{\mathbf{Y}} + (\mathbf{D} + v \mathbf{D}_{\text{Cor}}) \dot{\mathbf{Y}} + (\mathbf{S} + v^2 \mathbf{S}_{\text{in}}) \mathbf{Y} = F(t) \mathbf{w}_a, \tag{5}$$

where $\mathbf{M} = ((m + m_f) \delta_{ij} + M_a W_i(\xi_a) W_j(\xi_a))_{n \times n}$ is the mass matrix; $\mathbf{D} = (E^* I (\lambda_j / L)^4 \delta_{ij} + 2m_f v d_{ij})_{n \times n}$ – the damping matrix; $\mathbf{S} = (EI (\lambda_j / L)^4 \delta_{ij} + m_f v^2 a_{ij})_{n \times n}$ – the stiffness matrix; $\mathbf{w}_a = (W_1(\xi_a), \dots, W_n(\xi_a))^T$ – the vector of the eigenfunctions evaluated at the point where the actuators are attached, $F(t) = \frac{A}{\mu_0} (B_2^2 - B_1^2)$ – the magnetic force generated by the actuators, $a_{ij} = \int_0^L W_i W_j''$, $d_{ij} = \int_0^L W_i W_j'$, and δ_{ij} is Kronecker’s delta.

Reduce now the order of the problem by the substitution $x_i = Y_i$, $x_{n+i} = \dot{Y}_i$, $i = 1, 2, \dots, n$. The zero state will be a steady equilibrium when the induction is expressed as a deviation from the value in the middle position of the column: $x_{2n+1} = B_1 - B_0$, $x_{2n+2} = B_2 - B_0$, where $B_0 = \frac{\mu_0}{2z^* + l/\mu_r} \frac{NU}{R}$. We group the variables into vectors $\mathbf{x}_1 = (x_1, \dots, x_n)^T$, $\mathbf{x} = (x_1, \dots, x_{2n+2})^T$ and denote $\alpha = (\frac{AN^2}{R} + \frac{1}{8} \sigma l a^2)$, $\beta = \frac{\mu_0}{2z^* + l/\mu_r}$, $\gamma = \frac{NU}{R}$. The following nonlinear equations governing the dynamics of the whole system are then obtained

$$\dot{\mathbf{x}} = \mathbf{A}(\xi_a, U, v) \mathbf{x} + \mathbf{Q}(\mathbf{x}; \xi_a, U) = \mathbf{f}(\mathbf{x}; \xi_a, U, v), \tag{6}$$

with a matrix of the linear part

$$\mathbf{A}(\xi_a, U, v) = \begin{pmatrix} \mathbf{0} & \mathbf{I} & \mathbf{0} & \mathbf{0} \\ -\mathbf{M}^{-1} \mathbf{S} & -\mathbf{M}^{-1} \mathbf{D} & -\frac{2A}{\mu_0} \beta \gamma \mathbf{M}^{-1} \mathbf{w}_a & \frac{2A}{\mu_0} \beta \gamma \mathbf{M}^{-1} \mathbf{w}_a \\ -\frac{2}{\mu_0} \frac{\beta \gamma}{\alpha} \mathbf{w}_a^T & \mathbf{0} & -\frac{1}{\alpha \beta} & 0 \\ \frac{2}{\mu_0} \frac{\beta \gamma}{\alpha} \mathbf{w}_a^T & \mathbf{0} & 0 & -\frac{1}{\alpha \beta} \end{pmatrix} \tag{7}$$

and nonlinear terms

$$\mathbf{Q}(\mathbf{x}; \xi_a, U) = \begin{pmatrix} \mathbf{0} \\ \frac{A}{\mu_0} (x_{2n+2}^2 - x_{2n+1}^2) \mathbf{M}^{-1} \mathbf{w}_a \\ -\frac{2}{\alpha\mu_0} x_{2n+1} \mathbf{w}_a^T \mathbf{x}_I \\ \frac{2}{\alpha\mu_0} x_{2n+2} \mathbf{w}_a^T \mathbf{x}_I \end{pmatrix}. \quad (8)$$

It has been found that $n = 10$ base functions are sufficient to describe the pipe dynamics, while keeping the number of equations reasonably low for efficient optimization.

3 Numerical simulations

In this section the key dynamical features of the system and the effect of using actuators will be presented. All of the results are obtained by numerical simulations of the Galerkin system using the Runge-Kutta-Fehlberg method (RKF45) with adaptive selection of the step size. The solver estimates the discretization error at each step of the procedure and controls it by adjusting the step size until it achieves the desired accuracy in the solution, defined by the absolute error of 10^{-7} and the relative error of 10^{-6} .

When analyzing post-critical behavior of a similar system of Beck’s column with transformer actuators we obtained a good agreement between three approaches: (1) numerical integration of the continuous system (finite difference method applied to original PDE), (2) numerical simulations of the discretized system (RKF45 applied to ODE obtained using Galerkin’s method) and (3) theoretical bifurcation analysis of the discretized system [38]. Thus in the numerical part of this research we confined ourselves to simulations of the discretized system using the Fehlberg method.

Physical parameters are the same as in the actually built experimental set-up, see Table 1.

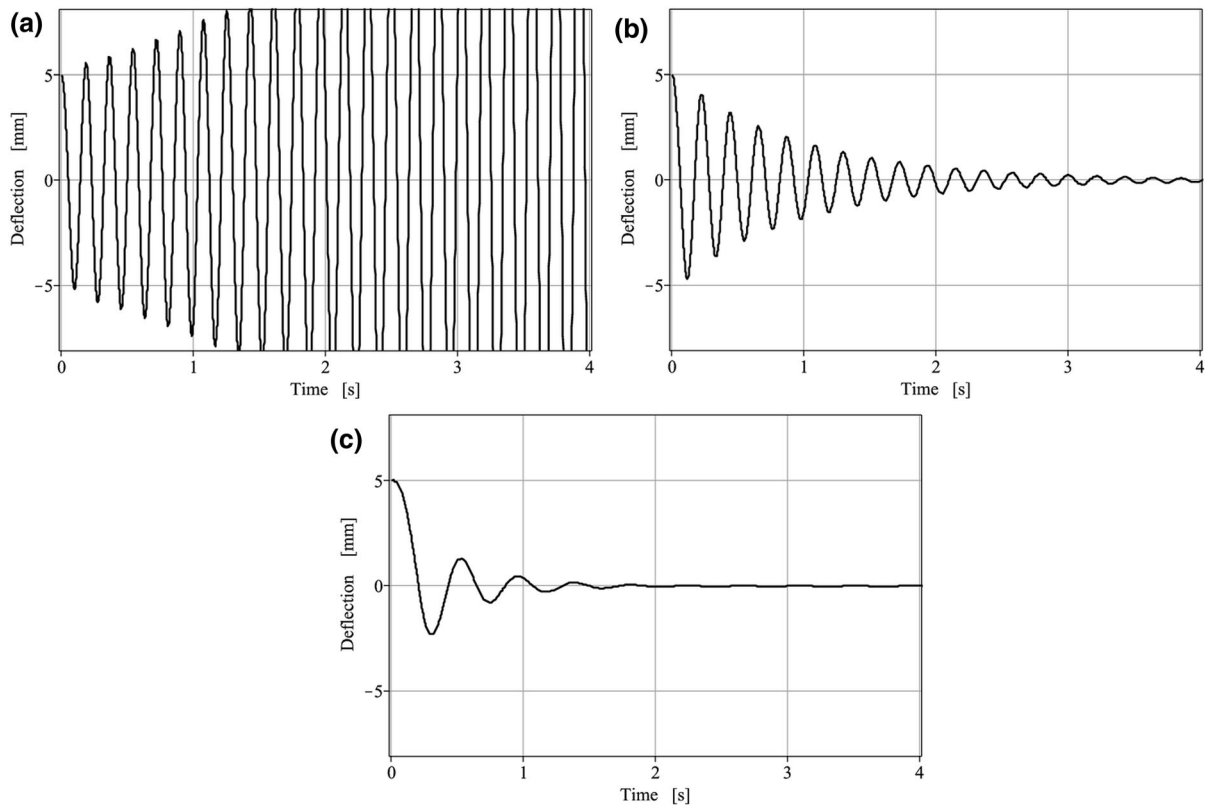
Note that due to many simplifications in the theoretical model (negligence of gravity force, thread restricting vibrations of the pipe to a plane, non-linear geometrical and material effects) and different position of the actuators, the results cannot be compared quantitatively. Still, qualitative features are alike.

In all numerical simulations the location of the actuators at $\xi_a = 0.6L = 576$ mm from the support is assumed. The reason for this choice will be explained a bit further. Initial deflection of the pipe amounts to 5 mm in the position $\xi_l = 555$ mm from the support and the figures show lateral deflection of this point. Begin with the time response of the pipe conveying air with velocity $v = 372$ m/s which is slightly above the critical value equal to $v_{cr} = 369.52$ m/s. In Fig. 2a one can observe that if no voltage is applied to the actuators, the system is unstable and vibrations grow exponentially. In reality, this motion would be limited by geometrical and material non-linearities or the width of gap in magnetic circuits but this model does not catch up these effects. Applying voltage to the actuators brings back the system stability, see Fig. 2b. When the voltage is further increased, the performance of the actuators improves, i.e. oscillations vanish quicker (Fig. 2c). However, one can observe that the period of vibrations extends, which is the result of the negative stiffness effect of the actuators. For values of voltage exceeding $U = 5$ V and actuators attached near the free end of the pipe, a small deflection of the system results in its divergence. i.e. losing stability of the straight equilibrium position. This is because the passively generated electromagnetic force outweighs the elastic force generated by the deflection of the pipe. If the actuators are closer to the pipe’s support, the system may be stable for higher values of voltage. However, the idea of the numerical analysis is to present critical flow velocity for all locations of the actuators along the pipe.

Now, we are going to focus on the actuators’ influence on the flow velocity leading to flutter. Figures 3 and 4 show the critical flow velocity for the system with no actuators attached to the pipe and for three selected values of voltage supplied to the actuators’ coils. Note the difference between curves “no actuators” and “ $U = 0$ ”. In the first case the system is reduced to a classical cantilever beam, in the other one – an effect of the lumped mass of the actuators is taken into account. The actuators are capable to increase the critical flow velocity, both due to their mass and the effect of electromagnetic force they generate. The latter is especially interesting in this research. Figure 3 illustrates that for various values of voltage the maxima of subsequent curves are around $\xi_a = 0.6L$. The exact locations could be

Table 1 Parameters of the examined system

Parameter	Unit	Value
Pipe length, L	m	0.960
Bending stiffness, EI	N·m ²	0.3194
Bending damping coefficient, E^*I	N·m ² ·s	0.000641
Pipe mass density, m	kg/m	0.0187
Fluid mass density, m_f	kg/m	0.000056
Magnetic circuit length, l	m	0.2
Magnetic circuit cross-section, $2a \times 2b$	m×m	0.01×0.01
Gap width, z^*	m	0.019
Mass of both actuators, M_a	kg	0.006
Coils number, N	–	210
Electric circuit resistance, R	Ω	1.40
Electrical conductivity of core, σ	1/(Ω ·m)	$3.8 \cdot 10^7$
Relative magnetic permeability of core, μ_r	–	18000
Magnetic permeability of vacuum, μ_0	H/m	$4\pi \cdot 10^{-7}$

**Fig. 2** Vibration of pipe with the flow of $v = 372$ m/s in the selected position $\xi_l = 555$ mm and various values of voltage; a) $U = 0$ V, b) $U = 3$ V and c) $U = 5$ V; $\xi_a = 0.6L$

calculated but they are all close enough to $0.6L$ to assume this position of actuators as the one for which their performance is close to the highest. Note that for

a range of actuators' positions around $1/4$ of pipe length or near the pipe end, their mass destabilizes the

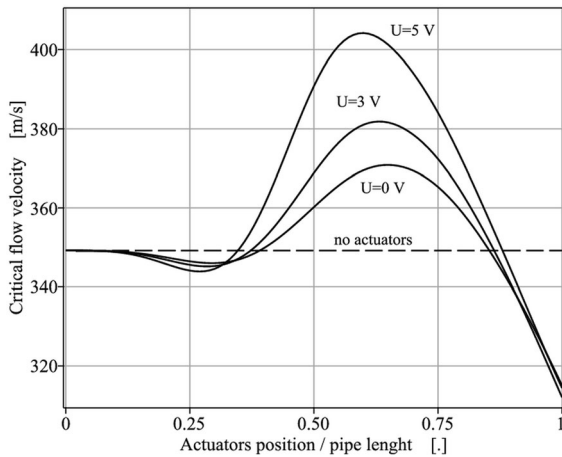


Fig. 3 Critical flow velocity as a function of actuators' position

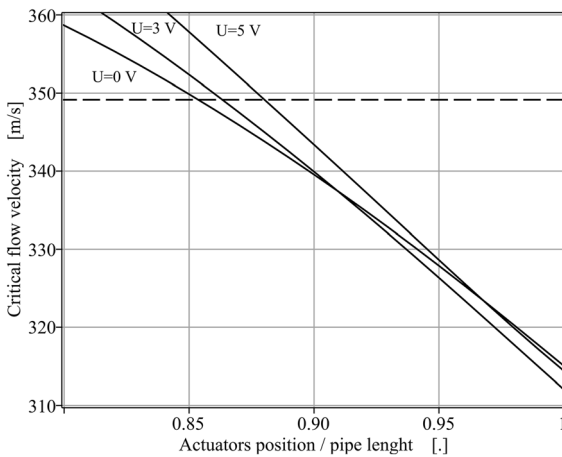


Fig. 4 Critical flow velocity as a function of actuators' position near the pipe end

system and the action of electromagnetic force makes this effect even more evident.

Figures 5 and 6 present the influence of flow velocity on the amplitude and frequency of post-critical flutter vibrations. These relations have been obtained by means of numerical simulations of the Galerkin system (6) for three selected values of voltage supplied to the actuators: $U = 1, 3$ and 5 V. Note that when no voltage is supplied to the actuators the dynamical equation of the system is a linear one, and for all values of the flow beyond the critical one the amplitude of flutter is infinite. Thus the simulations for $U = 0$ V have been disregarded in this study.

Numerical calculations were carried out for flow velocities exceeding the critical value by 0.01% ,

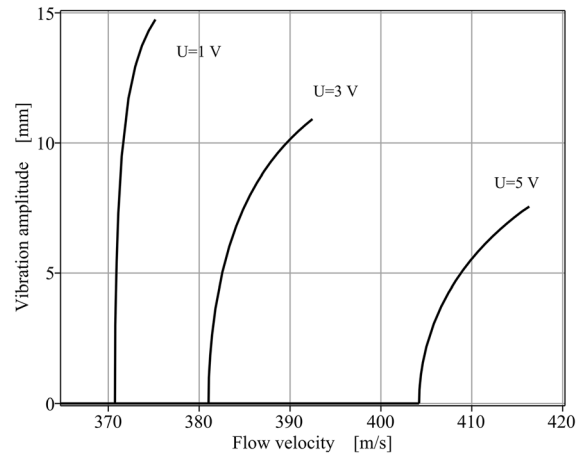


Fig. 5 Vibration amplitude measured at $\xi_l = 555$ mm as function of the flow velocity for selected values of voltage; $\xi_a = 0.6L$

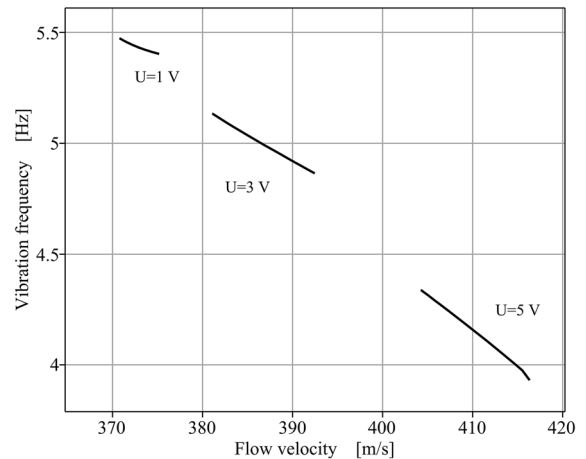


Fig. 6 Vibration frequency as function of the flow velocity for selected values of voltage; $\xi_a = 0.6L$

0.02% , 0.05% , 0.1% , 0.2% , and then with the step of 0.2% up to the value exceeding the critical one by 3% . For higher values of flow and some values of voltage either the amplitude of vibrations approached the limiting gap width z^* or the static action of the actuators overweighed the dynamical one and the pipe was permanently pulled towards one of the actuators. Observe that higher values of the post-critical flow velocities magnify the amplitude of flutter vibrations and decrease their base frequency.

The effect of magnetic force is for sure positive. Apart from increasing the critical flow velocity it leads to a smooth supercritical bifurcation. The increasing

voltage bends the bifurcating branches even further towards higher flows which means that the post-critical flutter amplitude is reduced. The actuators also exert a strong effect of reducing the initial frequency of flutter.

The existence of the soft-type of Hopf bifurcation has been proved by constructing the approximate periodic solution to Eq. (6) using the method proposed by Iooss and Joseph [18] and then calculating the Floquet coefficients of this solution for the analyzed in this section position of actuators and values of voltage. All coefficients are negative which means orbital stability of the limit cycle, i.e. a gradual increase of the amplitude of flutter vibration as the flow velocity grows beyond the critical value. These calculations will not be presented here because they are time-consuming and the scope of this work is the experimental validation of numerically predicted dynamics of the pipe with actuators. For details, please refer to the above mentioned work or, for example, [31, 38]. Note that the soft self-excitation was expected because it was also present in the case of Beck column with transformer actuators [38]. In linear approximation a pipe with flow differs from the Beck's column only by the additional term related to the Coriolis acceleration of the moving fluid, and the follower force is replaced with the square of the velocity of the flow.

4 Laboratory set-up

An experimental test stand has been designed and manufactured to verify theoretical analyses. Its

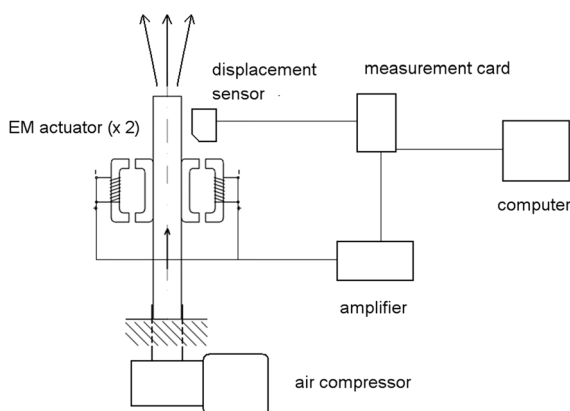


Fig. 7 Schematic of experimental set-up

simplified scheme is shown in Fig. 7. The experiments were conducted with pipes discharging fluid (i.e. moving it towards the free end) only. Generating flutter vibrations in a cantilever pipe moving fluid towards the support is much more cumbersome, and succeeded just several years ago [20]. Usually, the experiments have been conducted using liquids such as water or oil as a moving fluid, yet some of them involved air [3, 4, 17]. We followed the latter approach as it required neither sophisticated laboratory conditions nor large expenses. However, since such experiments are less typical than those using liquids, a correct choice of parameters related to pipe, air compressor and – in our case – electromagnetic actuators was necessary, i.e.:

- the test stand (especially: the air compressor and the power amplifier) meets the limitations given by the free space available in the laboratory and by the financial budget,
- the pipe is prone to flutter when the air starts flowing, yet still it is stiff enough to get the actuators attached,
- the actuators can generate electromagnetic force that is able to affect dynamics of the pipe, but the mass of the actuators does not disturb this dynamics too much.

The studied pipe is made of ABS styrene of density $\rho = 1.17 \text{ g/cm}^3$ with nominal length $L = 960 \text{ mm}$, external diameter $D = 9 \text{ mm}$ and internal diameter $d = 8 \text{ mm}$. The Young's modulus $E = 2.22 \text{ GPa}$ and the damping coefficient $E^* = 4.46 \text{ MPa}\cdot\text{s}$ of the material were determined during free vibration tests. The pipe was stuck by a grip handle to a composite wooden plate mounted on an aluminum truss frame. Conical shanks were used to connect the truss frame components, which ensured high stiffness of the structure by eliminating unnecessary clearances between truss elements. This prevented any unfavorable additional vibrations. The grip handle was connected to air compressor which allowed us to supply compressed air from the tank to pipe interior. Here, a fast pneumatic valve and a flow meter between the air compressor and the grip handle were used. An electromagnet was applied to impose a fixed initial deflection on the pipe. Along with a fast pneumatic valve, it was controlled by a real time unit, and they

were activated simultaneously to initiate the experimental trial.

To reduce the frequency of vibrations, additional mass was attached to the pipe. Moreover, the pipe was restrained by a thread so that vibrations would be planar. This approach already exists in the literature [3, 17]. Neither the additional mass nor the thread were incorporated in the model, which is another reason that the theoretical and experimental results cannot be directly compared. Still, the influence of additional mass and the thread (which can be treated as a spring) are known.

A view of the test stand is shown in Fig. 8 and its 3D CAD model is demonstrated in Fig. 9.

The scheme of measurement and current supply, and air distribution system installation is presented in Fig. 10.

It is based on a PC equipped with an I/O data acquisition card (NI PCI-6251), laser displacement sensors (OADM 12I6430/S35A made by Baumer) of maximum measurement resolution equal to 0.01 mm, a two-way current amplifier and electromagnetic devices of the transformer type (i.e. EM actuators). Initially, four laser sensors were used, however during the experiments it turned out that one sensor mounted at the height of $\xi_l = 555$ mm is sufficient to show the effect of the actuators. The constant control signal was magnified by an amplifier which was able to provide the

operating current of 0.1 . . . 5 A. This signal was sent to electromagnetic devices which generated damping force that acted on rectangular steel plates attached to the pipe. Each plate has dimensions of 89 mm x 22 mm x 0.25 mm, and is located at a distance of $\xi_a = 340$ mm from the support. Each of the C-shaped EM actuator was formed from iron, and along with the plates created a closed loop with an air gap. The width of the air gap amounted to $z^* = 19$ mm, and the cross-sectional dimensions of the actuator's core were 10×10 mm. The large value of the air gap enabled high-amplitude vibrations of the system. The coil was wound from an insulated aluminum wire of diameter 0.5 mm, which was wrapped 210 times around the core. The total length of the wire carrying current was approximately 10 m. The magnetic flux value in the gap was measured by the GM08 Gaussmeter made by Hirst Magnetic. This instrument has a measurement range of 0.0 . . . 3.0 T and a frequency range DC of 15 Hz . . . 10 kHz. The maximum induction of magnetic field used in the experiments was approximately 0.07 T, and the corresponding measured relative magnetic permeability of core was $\mu_r = 18000$.

Parameters of the system are listed in Table 1 in Sect. 3.

Note that for practical reasons in the experimental study the actuators were located at $\xi_a = 0.35L$ which is closer to the support than position $\xi_a = 0.60L$

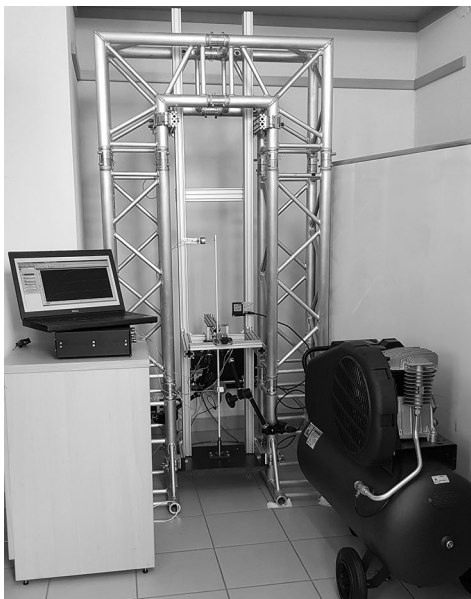


Fig. 8 Laboratory test rig of the standing cantilever pipe conveying air together with electromagnetic devices of transformer type

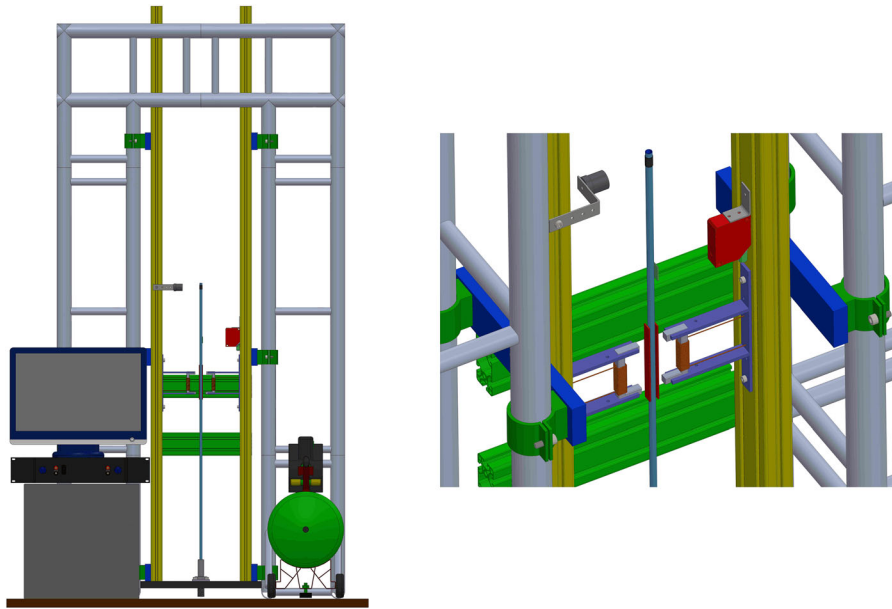


Fig. 9 The 3D CAD model of the considered system

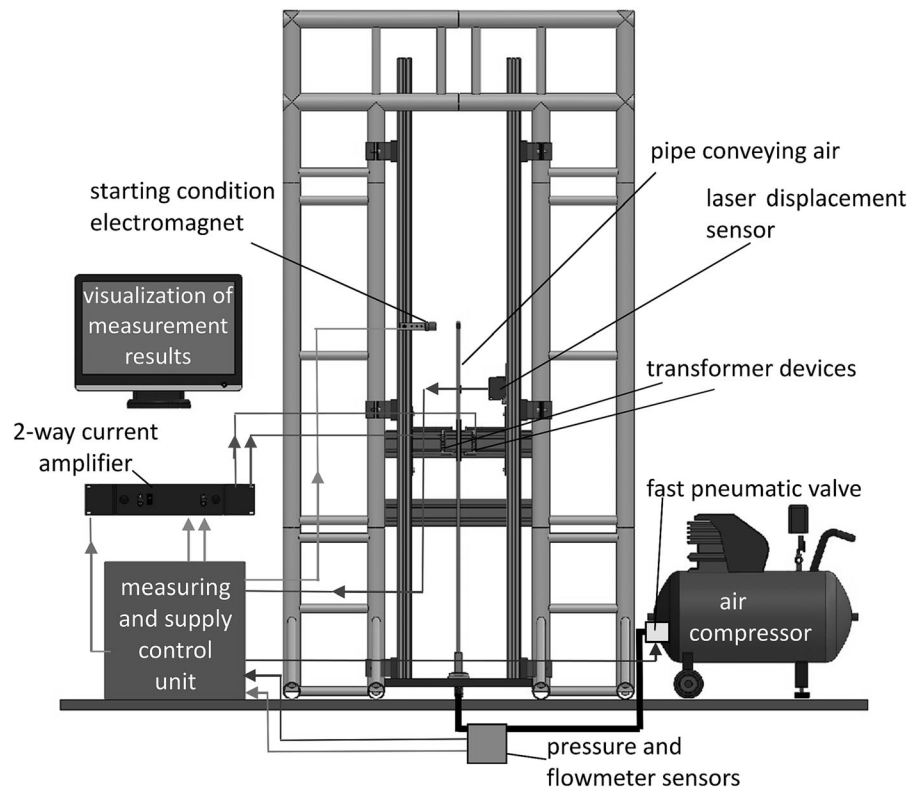


Fig. 10 Scheme of the measurement and the control system used in the test rig

suggested by the numerical analysis. Due to various imperfections of the experimental test stand – non-uniformity of the pipe’s material and geometry, variations in flow, necessity to stabilize vibration in a plane by an additional thread, unintended differences in actuators (both their cores and coils as well as the plates mounted on the pipe) – the oscillations were shifted from the vertical stable equilibrium and their amplitude changed in time. These problems became more and more pronounced as the actuators were moved towards the pipe’s end, because it happened that one of the actuators attracted the pipe resulting in divergence of the system or the amplitude was growing excessively resulting in break-up of the pipe. On the other hand, once the positive effect of the actuators located at 35% of the pipe’s length has been shown, one can expect even better performance at 60%, providing that the above mentioned technical problems are overcome.

5 Experimental results

The proposed stabilization method of the fluid-conveying pipe has been validated on the laboratory stand. The experiments were conducted for selected values of air pressure at the pipe’s inlet (which directly affects the flow velocity) and voltage supplied to the actuators’ coils. Note that the voltage could be higher than it was assumed in numerical simulations in Sect. 3 because the actuators were located closer to the support (35% of the pipe’s length instead of 60% used in numerical analysis) which enabled generating

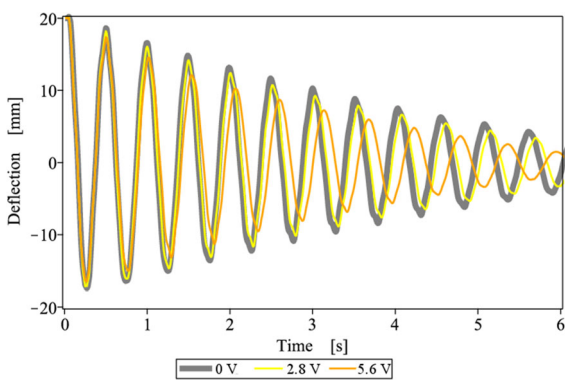


Fig. 11 Pipe deflection at height $\xi_l = 555$ mm for various values of voltage supplied to the actuators’ coils; no flow ($p = 0$ bar)

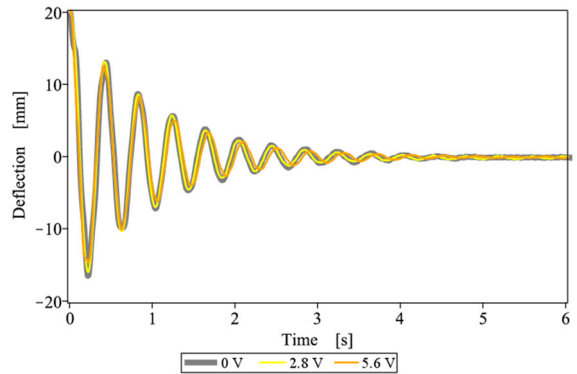


Fig. 12 Pipe deflection at height $\xi_l = 555$ mm for various values of voltage supplied to the actuators’ coils; moderate sub-critical flow ($p = 1$ bar)

higher electromagnetic force without the risk of divergence of the pipe. Figures 11, 12 and 13 show lateral deflection of the selected point on the pipe located at the distance of $\xi_l = 555$ mm.

Figure 11 presents a case with no air flow, so the pipe behaves exactly in the same way as a cantilever beam with additional mass of actuators’ plate added at the distance $\xi_a = 340$ mm from the support. Once electric current is supplied to the actuators, one can observe their action. The amplitude of vibration decreases quicker thanks to the dynamical stabilizing effect of the actuators, and the frequency of vibration is reduced due to negative stiffness introduced into the system by actuators.

In the case of moderate flow velocities generated by the static air pressure $p = 1$ bar at the pipe’s inlet the

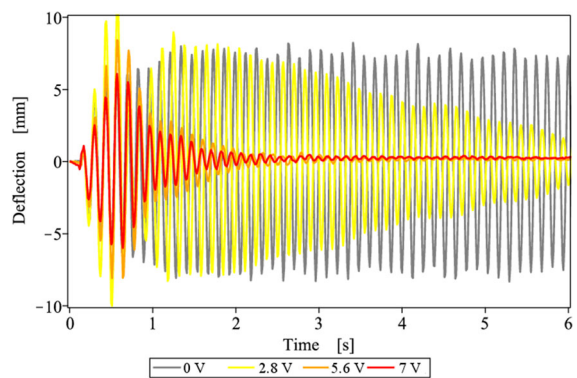


Fig. 13 Pipe deflection at height $\xi_l = 555$ mm for various values of voltage supplied to the actuators’ coils; slightly over-critical flow ($p = 2.8$ bar)

effect of actuators is less visible, see Fig. 12. This is because for such flows the damping effect of the Coriolis force is predominant in the system.

The most interesting effect is the ability of the actuators to increase the critical flow velocity (Fig. 13). The flow velocity is slightly beyond the critical one for the system with actuators turned off, which relates to air pressure $p = 2.8$ bar at the pipe's inlet. Turning the actuators on restores system stability. The efficiency of actuators grows with electric current in their coils, i.e. the system is stabilized faster, which confirms that the dynamical stabilizing effect of the actuators (increase of critical flow due to additional damping) dominates their passive destabilizing effect (decrease of critical flow due to negative stiffness introduced into the system).

A direct comparison between theoretical and experimental results is difficult for many reasons. The most important one is the location at which the actuators are attached to the pipe. In the numerical study we assumed the position close to the optimal in terms of increasing the critical flow velocity, whereas in the experimental study the actuators were located much closer to the support due to the reasons that have already been mentioned at the end of Sect. 4. Additionally, differences between numerical and experimental results come from various simplifications of the theoretical model presented in Sect. 3. The idea of the theoretical study was just to predict behavior of the pipe qualitatively, not quantitatively.

6 Conclusions

The influence of electromagnetic actuators of the transformer type on dynamics of a cantilever pipe discharging fluid was investigated. The dynamics of the system was examined in two ways. First, a dynamical model of the system was proposed and simulated numerically using Galerkin's approximation. Then, a specially designed and manufactured test stand was used to validate the results obtained in a numerical way.

The application of electromagnetic actuators of the transformer type can significantly improve the stability of the cantilever tube. The dynamic damping effect overweighs the static destabilization. The actuators are able to increase the critical flow velocity and reduce the amplitude of the post-critical flutter, if such occurs.

The effect of magnetic damping strongly depends on the position at which the actuators are attached to the pipe. The optimal location of the actuators is around 60% of the pipe's length, however for practical reasons other positions may be used too. The higher the voltage applied to the actuators the more evident the effect of negative stiffness, so the actual value should be selected carefully. An excessive voltage supplied to the coils may result in divergence of the system, i.e. losing stability of the straight equilibrium position. Thus the voltage should not exceed the value for which the passively generated electromagnetic force overweighs the elastic force resulting from deflection of the pipe. Since the growth of the resultant electromagnetic force is non-linear as a function of the lateral position of the pipe and the elastic force generated by the deflection of the pipe is a linear one, it would be enough to compare these forces for maximum deflection of the pipe. The elastic force comes from the classical Euler-Bernoulli beam theory, and the electromagnetic force is given by $A/\mu_0(B_2^2 - B_1^2)$, where the magnetic flux densities B_1 and B_2 can be calculated from two ordinary differential equations of magnetodynamics (1), assuming zero values of their rate of changes dB_1/dt and dB_2/dt . This calculation is obviously approximate due to simplifications of the model, but may be later tuned using measurements in the real system.

The proposed devices are contact-less, thus their application may be especially advisable for slender structures whose stability could be affected by the use of force actuators directly attached to the structure. Due to their construction, they can be easily adapted to changes of the working conditions. Moreover, a close-loop control of the system based both on static and dynamic magnetic forces can be devised.

Acknowledgements This research has been supported by the National Science Centre, Poland under grant agreement UMO-2015/17/D/ST8/02434.

Declaration

Conflict of interest The authors declare that they have no conflict of interest.

Open Access This article is licensed under a Creative Commons Attribution 4.0 International License, which permits use, sharing, adaptation, distribution and reproduction in any medium or format, as long as you give appropriate credit to the original author(s) and the source, provide a link to the Creative

Commons licence, and indicate if changes were made. The images or other third party material in this article are included in the article's Creative Commons licence, unless indicated otherwise in a credit line to the material. If material is not included in the article's Creative Commons licence and your intended use is not permitted by statutory regulation or exceeds the permitted use, you will need to obtain permission directly from the copyright holder. To view a copy of this licence, visit <http://creativecommons.org/licenses/by/4.0/>.

References

- Awrejcewicz J, Dzyubak LP (2010) 2-dof non-linear dynamics of a rotor suspended in the magneto-hydrodynamic field in the case of soft and rigid magnetic materials. *Int J Non-Linear Mech* 45(9):919–930
- Benjamin TB (1961) Dynamics of a system of articulated pipes conveying fluid. I. Theory. *Proc R Soc London Ser A Math Phys Sci* 261(1307):457–486
- Benjamin TB (1961) Dynamics of a system of articulated pipes conveying fluid. II. Experiments. *Proc R Soc London Ser A Math Phys Sci* 261(1307):487–499
- Chen SS (1985) Flow-induced vibration of circular cylindrical structures. Tech. Rep. ANL-85-51, Argonne National Lab. (ANL)
- Cui H, Tani J (1994) Flutter robust-control of a pipe conveying fluid. *Trans Japan Soc Mech Eng Ser C* 60(579):3789–3793
- Cui H, Tani J, Ohtomo K (1995) Robust flutter control of vertical pipe conveying fluid using gyroscopic mechanism. *Trans Japan Soc Mech Eng Ser C* 61(585):1822–1826
- Dai HL, Wang L (2015) Dynamics and stability of magnetically actuated pipes conveying fluid. *Int J Struct Stab Dyn* 16(06):1550026
- Dai J, Liu Y, Liu H, Miao C, Tong G (2019) A parametric study on thermo-mechanical vibration of axially functionally graded material pipe conveying fluid. *Int J Mech Mater Design* 15:716–726
- Doki H, Hiramoto K, Skelton R (1998) Active control of cantilevered pipes conveying fluid with constraints on input energy. *J Fluids Struct* 12(5):615–628
- Ebrahimi B, Bolandhemmat H, Khamesee MB, Golnaraghi F (2011) A hybrid electromagnetic shock absorber for active vehicle suspension systems. *Veh Syst Dyn* 49(1–2):311–332
- Eftekhari M, Hosseini M (2016) On the stability of spinning functionally graded cantilevered pipes subjected to fluid-thermomechanical loading. *Int J Struct Stab Dyn* 16(09):1550062
- Elishakoff I (2005) Controversy associated with the so-called “follower forces”: Critical overview. *Appl Mech Rev* 58(2):117–142
- Elishakoff I, Impollonia N (2001) Does a partial elastic foundation increase the flutter velocity of a pipe conveying fluid? *J Appl Mech* 68(2):206–212
- Fazelzadeh SA, Yazdanpanah B (2012) Active flutter suppression of thin-walled cantilever functionally graded piezoelectric pipes conveying fluid. In: 20th Annual International Conference on Mechanical Engineering-ISME2012, pp 1–4. School of Mechanical Eng., Shiraz University, Shiraz, Iran
- Graves KE, Toncich D, Iovenitti PG (2000) Theoretical comparison of motional and transformer emf device damping efficiency. *J Sound Vib* 233(3):441–453
- Gregory RW, Paidoussis MP (1966) Unstable oscillation of tubular cantilevers conveying fluid. I. Theory. *Proc R Soc Lond Ser A Math Phys Sci* 293(1435):512–527
- Gregory RW, Paidoussis MP (1966) Unstable oscillation of tubular cantilevers conveying fluid. II. Experiments. *Proc R Soc London Ser A Math Phys Sci* 293(1435):528–542
- Iooss G, Joseph D (1989) Elementary stability and bifurcation theory. Springer-Verlag, New York
- Khoshroo M, Eftekhari M (2021) Nonlinear behaviors of spinning pipes conveying fluid with pulsation. *Int J Struct Stab Dyn* 21:2150050
- Kuiper G, Metrikine A (2008) Experimental investigation of dynamic stability of a cantilever pipe aspirating fluid. *J Fluids Struct* 24:541–558
- Li Q, Liu W, Zhang Z, Yue Z (2018) Parametric resonance of pipes with soft and hard segments conveying pulsating fluids. *Int J Struct Stab Dyn* 18(10):1850119
- Li ZY, Wang JJ, Qiu MX (2016) Dynamic characteristics of fluid-conveying pipes with piecewise linear support. *Int J Struct Stab Dyn* 16(06):1550025
- Liang F, Gao A, Yang XD (2020) Dynamical analysis of spinning functionally graded pipes conveying fluid with multiple spans. *Appl Math Model* 83:454–469
- Lin YH, Chu CL (1996) Active flutter control of a cantilever tube conveying fluid using piezoelectric actuators. *J Sound Vib* 196(1):97–105
- Liu ZY, Wang L, Sun XP (2018) Nonlinear forced vibration of cantilevered pipes conveying fluid. *Acta Mech Solida Sin* 31(1):32–50
- Ma DM, Shiao JK (2011) The design of eddy-current magnet brakes. *Trans Can Soc Mech Eng* 35(1):19–37
- Paidoussis MP (1970) Dynamics of tubular cantilevers conveying fluid. *J Mech Eng Sci* 12(2):85–103
- Paidoussis MP (2008) The canonical problem of the fluid-conveying pipe and radiation of the knowledge gained to other dynamics problems across Applied Mechanics. *J Sound Vib* 310(3):462–492
- Pigolotti L, Mannini C, Bartoli G (2017) Destabilizing effect of damping on the post-critical flutter oscillations of flat plates. *Meccanica* 52(13):3149–3164
- Pisarski D, Konowrocki R, Szmidi T (2018) Dynamics and optimal control of an electromagnetically actuated cantilever pipe conveying fluid. *J Sound Vib* 432:420–436
- Przybyłowicz PM, Kurnik W (2020) Stability and bifurcation analysis of an overhung rotor with electromagnetic actuators. *J Theor Appl Mech* 58(2):525–539
- Schweitzer G, Maslen EH (2009) Magnetic bearings. Springer-Verlag, Berlin Heidelberg
- Sugiyama Y, Kumagai Y, Kishi T, Kawagoe H (1986) Studies on stability of pipes conveying fluid (the effect of a lumped mass and damping). *Bull JSME* 29(249):929–934
- Sugiyama Y, Tanaka Y, Kishi T, Kawagoe H (1985) Effect of a spring support on the stability of pipes conveying fluid. *J Sound Vib* 100:257–270

35. Sun X, Yan H, Dai H (2020) Stability and dynamic evolution of sliding fluid-transporting pipes in three-dimensional sense. *Int J Struct Stab Dyn* 20(03):2050036
36. Szmids T, Pisarski D, Konowrocki R (2019) Semi-active stabilisation of a pipe conveying fluid using eddy-current dampers: state-feedback control design, experimental validation. *Meccanica* 54(6):761–777
37. Szmids T, Przybyłowicz P (2013) Critical flow velocity in a pipe with electromagnetic actuators. *J Theor Appl Mech* 51(2):487–496
38. Szmids T, Przybyłowicz P (2014) Critical load and non-linear dynamics of Beck's column with electromagnetic actuators. *Int J Non-Linear Mech* 67:63–73
39. Tang Y, Yang T, Fang B (2018) Fractional dynamics of fluid-conveying pipes made of polymer-like materials. *Acta Mech Solida Sin* 31(2):243–258
40. Tani J, Sudani Y (1995) Active flutter suppression of a vertical pipe conveying fluid. *JSME Int J Ser C Dyn Control Robot Design Manuf* 38(1):55–58
41. Tonoli A, Amati N, Silvagni M (2010) Electromechanical dampers for vibration control of structures and rotors. In: M Lallart (ed.) *Vibration Control*, pp 1–32. Sciyo . Available from: <https://www.intechopen.com/books/vibration-control-of-structures-and-rotors>
42. Tsai YK, Lin YH (1997) Adaptive modal vibration control of a fluid-conveying cantilever pipe. *J Fluids Struct* 11(5):535–547
43. Wang L, Ni Q (2008) Large-amplitude free vibrations of fluid-conveying pipes on a pasternak foundation. *Int J Struct Stab Dyn* 08(04):615–626
44. Zhou XW, Dai HL, Wang L (2018) Dynamics of axially functionally graded cantilevered pipes conveying fluid. *Compos Struct* 190:112–118
45. Zuo L, Bae JS, Hwang JH, Kwag DG, Park J, Inman DJ (2014) Vibration suppression of a large beam structure using tuned mass damper and eddy current damping. *Shock Vib* 2014(893914):1–10

Publisher's Note Springer Nature remains neutral with regard to jurisdictional claims in published maps and institutional affiliations.